
Learning to Explore with Parameter-Space Noise: A Deep Dive into Parameter-Space Noise for Reinforcement Learning with Verifiable Rewards

Bizhe Bai^{1,2} Xinyue Wang¹ Peng Ye^{3,4} Tao Chen^{2,1}

Abstract

Reinforcement Learning with Verifiable Rewards (RLVR) improves LLM reasoning, yet growing evidence indicates an *exploration ceiling*: it often reweights existing solution traces rather than discovering new strategies, limiting gains under large sampling budgets (e.g., `pass@256`). We address this limitation with **PSN-RLVR**, which perturbs policy parameters *before* rollout generation to induce temporally consistent, trajectory-level exploration that better preserves long-horizon chain-of-thought coherence than action-space noise. To mitigate the induced sampling–update mismatch, we incorporate **truncated importance sampling** (TIS), and to avoid expensive KL-based adaptive noise control, we propose a **computationally efficient** real-time adaptive noise scheduler driven by a lightweight surrogate that combines semantic diversity with normalized self-certainty. Instantiated on **GRPO**, a widely used RLVR method, **PSN-GRPO** consistently expands the effective reasoning capability boundary across multiple mathematical reasoning benchmarks and model families, yielding higher `pass@k` under large sampling budgets and outperforming prior exploration-oriented RLVR methods (e.g., `Pass@k`-style training) while remaining *orthogonal* and thus composable for additional gains.

1. Introduction

Reinforcement Learning with Verifiable Rewards (RLVR) has become a central paradigm for improving the reasoning behaviors of Large Language Models (LLMs), delivering substantial gains on domains with automatic correct-

ness signals such as mathematics and code generation (Lu et al., 2024; Ouyang et al., 2022; Lambert et al., 2025). In this setting, policy-gradient style algorithms—most notably Proximal Policy Optimization (PPO) (Schulman et al., 2017) and its recent variants such as Group Relative Policy Optimization (GRPO) (Guo et al., 2025)—enable direct optimization against verifiers (e.g., unit tests or symbolic checkers), aligning models with ground-truth correctness and propelling systems like DeepSeek-R1 (Guo et al., 2025) to strong empirical performance. However, emerging evidence suggests that current RLVR pipelines may face an *exploration ceiling*. Recent analyses (Yue et al., 2025; Wu et al., 2026) indicate that RLVR tends to improve *sampling efficiency* (i.e., `pass@1`) rather than inducing genuinely new reasoning capability boundaries (i.e., `pass@256`): the trajectories produced after RLVR are largely contained within (or near) the base model’s pretraining distribution. In addition, the RLVR-trained LLM tend to have less semantic diversity and operation diversity compared to the original model (Dang et al., 2025) as shown in Figure 1 (right). Under this view, RLVR behaves primarily as a distributional *reweighting* mechanism—it amplifies pre-existing correct trajectories while rarely discovering qualitatively new solution strategies. This leaves an “exploration gap”: the inability to reliably traverse regions of the reasoning space that are unlikely under the initial policy but may contain superior or more robust solutions.

Bridging this gap requires balancing exploration (Sutton & Barto, 1998) and exploitation while preserving the long-horizon dependency essential for Chain-of-Thought (CoT) reasoning. Existing approaches generally fall into three categories, each with distinct limitations: **1. Action-Space Perturbations (Decoding-Time)**: Techniques such as temperature sampling (Renze & Guven, 2024) or nucleus sampling (Holtzman et al., 2019) inject stochasticity at the token level. However, token-level noise is typically *uncorrelated* across time steps. In multi-step reasoning, small perturbations in each step may accumulate into unstructured noise that degrades global coherence, harming long-horizon reasoning trajectories (Renze & Guven, 2024), rendering the CoT state-level inconsistent. **2. Objective-Level Regularization**: Methods that modify the training objective—such as entropy bonuses (Zhan et al., 2025) or `pass@k` optimization

¹College of Future Information Technology, Fudan University, Shanghai, China ²Shanghai Innovation Institute, Shanghai, China ³Shanghai AI Laboratory, Shanghai, China ⁴The Chinese University of Hong Kong, Hong Kong, China. Correspondence to: Bizhe Bai <bizhe.bai@sii.edu.cn>, Tao Chen <eetchen@fudan.edu.cn>.

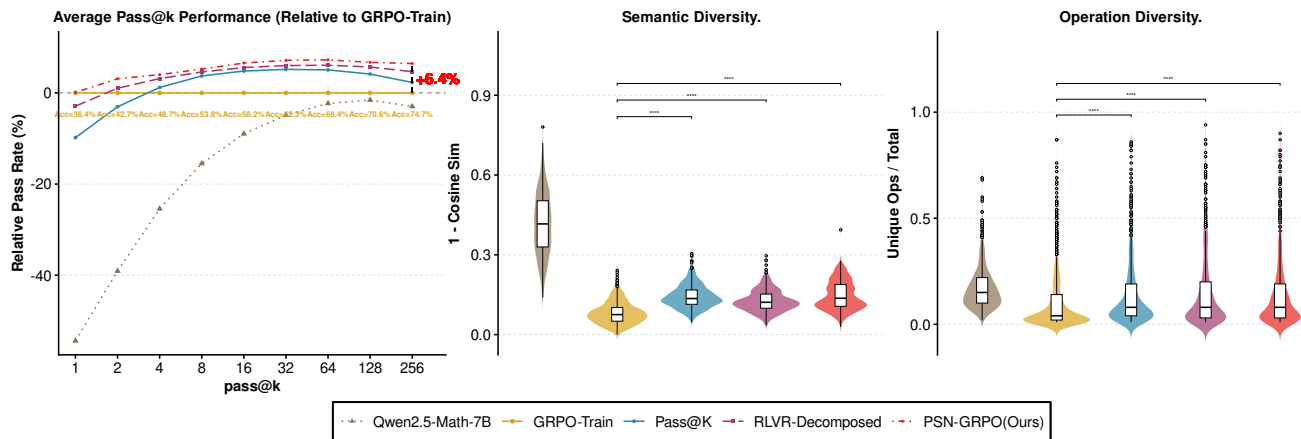


Figure 1. Comparison of reasoning capability boundaries across different RLVR paradigms. (1) Standard RLVR-trained models (GRPO-Train) exhibit a significant reduction in **semantic diversity** and **operation diversity** compared to the base model (Qwen2.5-Math-7B). (2) Our proposed method, **PSN-GRPO**, restores and enhances this diversity, achieving significantly higher semantic and operation variance compared to the GRPO baseline. (3) In terms of reasoning performance, PSN-GRPO is superior to other exploration-focused methods, such as **Pass@k training** (Chen et al., 2025) and **RLVR-Decomposed** (Zhu et al., 2025), consistently delivering higher **pass@k** metrics, particularly under large sampling budgets (e.g., $k = 128, 256$).

(Chen et al., 2025)—attempt to force diversity explicitly. **3. Data Augmentation:** While experience augmentation (e.g., self-generated task variants, offline data, or external teacher models) (Liang et al., 2025; Dong et al., 2025; Li et al., 2025) can broaden support but often introduces additional computational cost or reliance on external signals. More discussion is provided in Section 2.2.

To overcome these limitations, we propose **PSN-RLVR**, a parameter-space exploration framework for RLVR that perturbs policy parameters prior to rollout generation, inducing *temporally consistent*, trajectory-level exploration better aligned with long-horizon chain-of-thought reasoning than token-level noise. Beyond introducing PSN to RLVR, we *comprehensively explore* its design space in this setting (Section 4.2), systematically characterizing where to inject noise, how performance scales with noise magnitude, when PSN is preferable to action-space perturbations, and how PSN interacts with existing RLVR exploration techniques. Applying PSN in RLVR poses two unique challenges—off-policy sampling–update mismatch and compute-aware noise control—which we address with two lightweight modules: (i) **truncated importance sampling (TIS)** to stabilize optimization under rollouts collected from the perturbed sampler, and (ii) a **real-time adaptive noise scheduler** that replaces expensive KL-based control with a low-overhead surrogate combining semantic diversity and normalized self-certainty. Instantiated on GRPO, PSN-RLVR consistently expands the effective reasoning capability boundary, improving **pass@k** under large sampling budgets while remaining orthogonal and composable with prior RLVR enhancements.

To the best of our knowledge, this paper presents the **first systematic study of parameter-space noise** for Large Lan-

guage Models trained with Verifiable Rewards (RLVR). Our main contributions are:

- **PSN-RLVR: parameter-space exploration for RLVR.** We introduce a parameter-space noise framework for RLVR that perturbs policy parameters before rollout generation to induce temporally consistent, trajectory-level exploration, and instantiate it on GRPO to form **PSN-GRPO**.
- **Two modules for RLVR-specific challenges.** To address the sampling–update mismatch induced by parameter perturbations, we incorporate **truncated importance sampling (TIS)** for stable off-policy learning; to avoid expensive KL-based noise control, we propose a **lightweight real-time adaptive noise scheduler** driven by a surrogate that combines semantic diversity and model’s self-certainty.
- **Comprehensive exploration of the PSN design space in RLVR.** We conduct extensive experiments and targeted ablations (Section 4.2) that systematically answer key design questions—noise injection location, noise magnitude scaling, robustness across model families, comparisons to action-space noise, and complementarity with other exploration-oriented RLVR methods—demonstrating consistent improvements in high-budget **pass@k** and reasoning diversity.

2. Related Work

2.1. Reinforcement Learning for Reasoning with Verifiable Rewards

The integration of Reinforcement Learning (RL) into the post-training pipeline of Large Language Models (LLMs) has become a standard paradigm for enhancing performance in domains with objective ground-truth, such as mathematics and coding (Ouyang et al., 2022; Lu et al., 2024; Guo et al., 2025). More discussion in Appendix A.

2.2. The Exploration-Exploitation Boundary in LLMs

Existing approaches generally fall into three categories (1) Action-Space Perturbations (Decoding-Time) (2) Objective-Level Regularization (3) Data Augmentation. We provide detailed summary of three classes and state their distinct limitations in following. First, a large class of methods modulates exploration at *decoding time* by perturbing the action space—e.g., temperature sampling (Renze & Guven, 2024), nucleus/top- k sampling (Holtzman et al., 2019), or prompt perturbations (Shur-Ofry et al., 2024). Although these heuristics can increase diversity, they typically demand careful hyperparameter tuning (Du et al., 2025) and can be sensitive across domains and model families (Shi et al., 2024; Qiang et al., 2024; Chen et al., 2024). More fundamentally, token-level stochasticity is often *locally uncorrelated* across time (Renze & Guven, 2024), so small perturbations can accumulate into unstructured jitter that reduces long-horizon CoT coherence, derailing global logical consistency in difficult reasoning trajectories.

Second, training-time diversification can be pursued by modifying the RLVR objective, such as substituting the pass@1 objective with pass@ k objectives (Chen et al., 2025; Peng et al., 2025) in GRPO (Guo et al., 2025), using output entropy as a proxy for exploration control (Cheng et al., 2025a; Cui et al., 2025), or incorporating negative samples to promote exploration (Zhu et al., 2025). While promising, objective-level regularization often depends on proxy signals whose effectiveness can be sensitive to task difficulty and reward sparsity.

Third, another line of work relies on data and experience augmentation to broaden exploration, such as creating new task variations from the model itself (Liang et al., 2025), leveraging off-line data (Dong et al., 2025; Li et al., 2025), or using additional LLM guidance (Jiang et al., 2025). Although these approaches can expand the effective support of training, they typically bring additional computation cost, require extra data curation, or introduce external signals beyond the base RLVR loop.

2.3. Parameter-Space Noise

Parameter-Space Noise (PSN) offers another compelling alternative by perturbing the policy weights rather than the actions. Works such as (Plappert et al., 2018) and (Fortunato et al., 2018) demonstrated in continuous control domains that PSN induces state-dependent exploration: a perturbed policy acts as a distinct "agent" that executes a consistent strategy over an entire episode. While PSN is well-established in robotics (Fortunato et al., 2018; Gupta et al., 2018; Hollenstein et al., 2022; Gravell & Summers, 2021), its application to the discrete, high-dimensional reasoning space of RLVR remains largely unexplored. On the other side, subsequent theoretical work situates such noise-injected policies within the broader paradigm of posterior sampling / randomized value functions, which can induce deep exploration and admits regret guarantees (Osband et al., 2019; Russo, 2019). In particular, variational Thompson-sampling perspectives interpret practical parameter-noise methods as tractable approximations to posterior sampling over value functions, providing a theoretical foundation for their empirical effectiveness (Aravindan & Lee, 2021).

A concurrent work is QERL (Huang et al., 2025), which focuses on improving RLVR training efficiency via quantization. While they report that the noise introduced by quantization *surprisingly* improved exploration, this phenomenon was observed as side effect of their efficiency optimization. Consequently, they did not systematically analyze the noise dynamics, optimal injection strategies, or scaling laws required to leverage this effect for reasoning.

3. Methodology

3.1. Preliminaries: Group Relative Policy Optimization

We build our framework upon Group Relative Policy Optimization (GRPO) (Guo et al., 2025), a widely used RLVR method, which optimizes a policy π_θ without a value function. For each query $q \sim P(Q)$, GRPO samples a group of outputs $\{o_i\}_{i=1}^G$ from the old policy $\pi_{\theta_{\text{old}}}$ and optimizes the following objective:

$$\mathcal{J}_{\text{PPO}}(\theta) = \mathbb{E}_{q \sim P(Q), o \sim \pi_{\theta_{\text{old}}}(O|q)} \left[\frac{1}{|o|} \sum_{t=1}^{|o|} \ell_t^{\text{clip}}(\theta) \right], \quad (1)$$

where $\ell_t^{\text{clip}}(\theta) = \min(r_t(\theta)A_t, \text{clip}(r_t(\theta), 1 - \varepsilon, 1 + \varepsilon)A_t)$, and $r_t(\theta) = \frac{\pi_\theta(o_t|q, o_{<t})}{\pi_{\theta_{\text{old}}}(o_t|q, o_{<t})}$ where A_t is the advantage computed from relative rewards within the group.

3.2. Parameter-Space Noise GRPO (PSN-GRPO)

We initialize PSN-RLVR with PSN-GRPO, an exploration-enhanced training framework that injects parameter-space noise into the rollout policy to induce temporally consistent

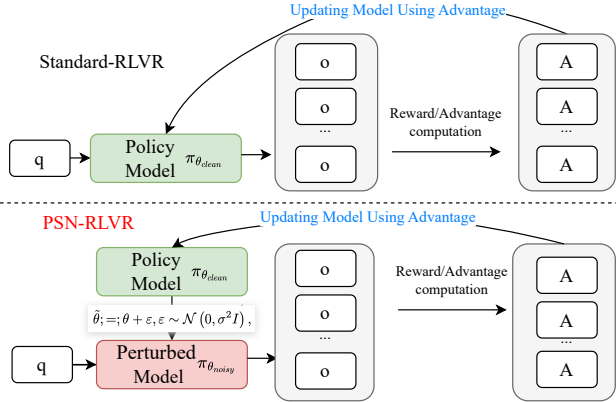


Figure 2. Overview of the PSN-RLVR framework compared to Standard-RLVR. The noise-perturbed model $\pi_{\tilde{\theta}}$ generates rollouts to induce temporally consistent, trajectory-level exploration. The resulting reward signals are used to update the clean policy π_{θ}

exploration while updating the clean policy parameters via policy gradient learning. Because rollouts are generated by a noisy sampler policy, we correct the resulting off-policy mismatch using Truncated Importance Sampling (TIS). Finally, we propose a computationally efficient, real-time scheduler for noise. The main framework is illustrated in Figure 2.

3.3. Parameter-space noise exploration policy

Following Plappert et al. (2018), we explore by perturbing parameters rather than actions/tokens. At the beginning of each iteration, we apply additive Gaussian noise to the parameter vector of the current policy :

$$\tilde{\theta}; =; \theta + \varepsilon, \varepsilon \sim \mathcal{N}(0, \sigma^2 I), \quad (2)$$

which induces a *noisy exploration policy* $\pi_{\tilde{\theta}}$. Crucially, $\tilde{\theta}$ is held fixed for the entire rollout, yielding temporally consistent exploration: conditioned on the same prefix $(q, o_{<i>i$

3.4. Off-Policy Correction via Truncated Importance Sampling

A distribution mismatch arises because data is collected by $\pi_{\tilde{\theta}}$ but used to train π_{θ} . Ignoring this discrepancy yields biased gradient estimates. We correct this via Truncated Importance Sampling (TIS) (Ionides, 2008). We modify the standard GRPO objective by incorporating the importance ratio w_t into the gradient update. The corrected objective is:

$$\mathcal{J}_{\text{PSN}}(\theta) = \mathbb{E}_{q \sim P(Q), o \sim \pi_{\tilde{\theta}}} \left[\frac{1}{|o|} \sum_{t=1}^{|o|} w_t \cdot \ell_t^{\text{clip}}(\theta) \right]. \quad (3)$$

To prevent unbounded variance when $\pi_{\tilde{\theta}}$ diverges significantly from π_{θ} , we truncate the importance ratio:

$$w_t := \min\left(\frac{\pi_{\theta}(a_t)}{\pi_{\tilde{\theta}}(a_t)}, C\right) \quad (4)$$

where C is a clipping hyperparameter. This formulation allows the learner to leverage exploratory data from $\pi_{\tilde{\theta}}$ while maintaining training stability.

3.5. Adaptive Noise Scheduling

We would like the exploration policy to remain sufficiently close to the learner to keep off-policy correction stable, while still being different enough to encourage exploration. We therefore measure how far the noisy policy deviates from the clean policy on the *current* batch and adjust the noise for the *next* batch. We propose two adaptive scaling variants to dynamically adjust σ .

3.5.1. VARIANT I: NON-REAL SCHEDULER

Following (Plappert et al., 2018), we adjust σ to maintain a target KL divergence, δ_{KL} , between the clean and noisy policies. After each batch, we compute:

$$d(\pi_{\theta}, \pi_{\tilde{\theta}}) = \mathbb{E}_s [\text{KL}(\pi_{\tilde{\theta}}(\cdot|s) \parallel \pi_{\theta}(\cdot|s))]. \quad (5)$$

The noise scale for the next iteration, σ_{k+1} , is updated via:

$$\sigma_{k+1} = \begin{cases} \beta \sigma_k & \text{if } d(\pi_{\theta}, \pi_{\tilde{\theta}}) \leq \delta_{\text{KL}} \\ \frac{1}{\beta} \sigma_k & \text{otherwise,} \end{cases} \quad (6)$$

where $\beta > 1$ is a step constant. However, this retrospective adaptation introduces feedback latency. Given the high variance in problem difficulty within RLVR datasets, this lag can lead to suboptimal noise scheduling: high noise levels necessitated by a difficult problem batch may be inappropriately applied to a subsequent simple problem batch, causing a mismatch that hinders efficient training.

3.5.2. VARIANT II: REAL-TIME COMPUTATIONALLY EFFICIENT SCHEDULER

To address the feedback lag and computational cost of full rollout sampling, we propose a real-time scheduler based on *semantic diversity* and *model self-certainty*. For each query q , we pre-generate two probe rollouts $o^{(1)}, o^{(2)}$ using the clean policy π_{θ} to gauge the model’s current exploration needs.

Motivation. Ideally, accurate noise calibration for the current batch would require computing $d(\pi_{\text{clean}}, \pi_{\text{noisy}})$ *a priori*. However, this is computationally prohibitive. Since rollout generation accounts for 70–80% of total training time (Cheng et al., 2025b), a naive approach—sampling a set of rollouts (e.g., $N = 8$) to measure divergence, adjusting noise, and then resampling for backpropagation—would nearly double the computational overhead. To circumvent this, we propose a computationally efficient schedule that calibrates noise based on immediate signals of *semantic similarity* and *model self-certainty*. To this end, for each query q , we pre-generate two rollouts, $o^{(1)}$ and $o^{(2)}$, using π_{clean} to compute indicators based on semantic embeddings (Dang

et al., 2025) and self-certainty (Kang et al., 2025). We explicitly avoid using $KL(\pi_{\text{clean}}||\pi_{\text{noisy}})$ for this adjustment because “KL between language models notoriously suffers from high variance” (Amini et al., 2025; Fang et al., 2025), particularly when estimated from only two samples.

Semantic similarity. Let $f(\cdot)$ be a fixed sentence embedding model; we compute

$$d_{\text{sem},i} = \cos(f(o^{(1)}), f(o^{(2)})), \bar{d}_{\text{sem},t} = \frac{\sum_1^B d_{\text{sem},i}}{B} \quad (7)$$

where B is batch size, and $\bar{d}_{\text{sem},t}$ is mean of semantic similarity of current batch. Higher similarity indicates models tend to generate similar rollouts, signaling a need for greater exploration (i.e., larger parameter noise).

Self-Certainty. We quantify *distributional self-certainty* by measuring how far the model’s token-level predictive distribution departs from a uniform prior over the vocabulary. The key intuition is that a sharper (more concentrated) distribution corresponds to greater confidence. Concretely, for a query q and a generated completion $o = (o_1, \dots, o_{|o|})$, let U be the uniform distribution on the vocabulary V . We define self-certainty as the mean, across decoding steps, of the KL divergence from U to the model distribution p_{π_θ} :

$$\text{Self-certainty}(o | q) = \frac{1}{|o|} \sum_{i=1}^{|o|} \text{KL}(U || p_{\pi_\theta}(\cdot | q, o_{<i})), \quad (8)$$

where $o_{<i}$ are the previously generated tokens and $p(j | q, o_{<i})$ is the model’s predicted probability for token j at step i . Higher self-certainty values indicate greater confidence. Larger values imply stronger concentration of probability mass, i.e., greater deviation from uniformity and thus requiring more exploration. We normalize the batch-averaged self-certainty SC_t to $[0, 1]$ using a global history buffer of running extrema (S_{\min}, S_{\max}) :

$$\bar{\text{SC}}_t^{\text{norm}} = \text{clip}\left(\frac{\text{SC}_t - S_{\min}}{S_{\max} - S_{\min} + \epsilon}, 0, 1\right). \quad (9)$$

Update Rule. We define a composite indicator $\text{Ind}_t = \bar{\text{SC}}_t^{\text{norm}} + \bar{d}_{\text{sem}}$ for current batch. A high Ind_t implies the model is both confident and producing semantically similar outputs, signaling a need for stronger perturbations. We compare Ind_t to its historical mean $\bar{\text{Ind}}$ to update σ :

$$\sigma_k = \begin{cases} \beta \sigma_{k-1} & \text{if } \bar{\text{Ind}} \leq \text{Ind}_t \\ \frac{1}{\beta} \sigma_{k-1} & \text{otherwise} \end{cases} \quad (10)$$

Compute overhead. Variant II uses two probe generations per query. Empirically, we observe a smaller end-to-end throughput reduction of $\approx 8\%$ relative to fixed- σ PSN under identical hardware. We attribute the gap to *generation-time imbalance* (He et al., 2025). More discussion is illustrated in Appendix C.

4. Experiments

4.1. Experimental setup

Training, Models, and Datasets. We adopt GRPO (Guo et al., 2025) as the default RLVR training algorithm. Unless otherwise specified, all experiments utilize the standard configuration of SimpleRL-Zoo¹ (Zeng et al., 2025), including learning rate, batch size, rollout count, and maximum sequence length; detailed hyperparameters are provided in Appendix B. We test our method on Qwen2.5-Math-7B (Yang et al., 2024) and Qwen2.5-7B (Team, 2025b). Following the SimpleRL-Reason protocol (Zeng et al., 2025), training data is sampled from the NuminaMath dataset (LI et al., 2024), which is derived from GSM8K (Cobbe et al., 2021) and MATH (Hendrycks et al., 2021). Unless explicitly stated otherwise, all reported results rely on the Qwen2.5-Math-7B model trained under these default settings.

Evaluation Protocol. Evaluations are conducted on a variety of reasoning benchmarks: AIME 2024, AIME 2025, AMC 2023 (aim, 2025), OlympiadBench (He et al., 2024), and Minerva Math (Lewkowycz et al., 2022). To ensure a fair and consistent comparison, all our evaluation framework is built upon the open-source simpleRL-reason codebase (Zeng et al., 2025). To obtain a comprehensive evaluation, we adopt the unbiased pass@ K metric with K up to 256, computed as $\text{pass}@K := \mathbb{E}_{x \sim \mathcal{D}}[1 - \binom{n-c}{K} / \binom{n}{K}]$, where c denotes the number of correct completions out of n generated responses following (Peng et al., 2025). To reduce evaluation variance, we set $n = 300$ for all datasets. Unless otherwise specified, we use a decoding temperature $T = 0.9$ for all evaluation tasks.

Metrics representing reasoning capability boundary.

We use two metrics for representing reasoning capability boundary of RLVR (1) pass@ k following by (Yue et al., 2025; Peng et al., 2025; Chen et al., 2025) (2) semantic embedding diversity and operation diversity between LLM’s rollouts following by (Dang et al., 2025). Semantic Diversity: the average cosine similarity between the text embeddings of the rollouts, computed using Bert-MLM_arXiv-MP-class_zbMath (Steinfeldt & Mihaljevic, 2024). Operation Diversity: group rollouts by the sequence of arithmetic operations performed and measure the fraction of unique operation sequences.

4.2. Results and Q&As

We present our results via the following Q&As.

Q1: Does PSN-RLVR expand the reasoning capability boundary?

¹<https://github.com/hkust-nlp/simpleRL-reason>

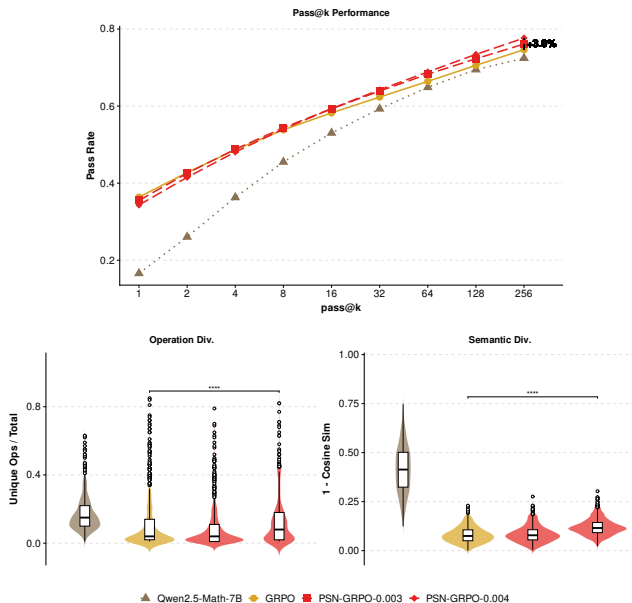


Figure 3. We compare the pass@ k performance (top), semantic diversity, and operation diversity of PSN-GRPO against the standard GRPO baseline on Qwen2.5-Math-7B. PSN-GRPO achieves superior performance at large sampling budgets ($k \geq 16$). This gain is strongly correlated with increased semantic and operational diversity in generated trajectories (Dang et al., 2025).

A: Yes, PSN-RLVR achieves higher pass@ k under large sampling budgets and increased rollouts semantic diversity and operation diversity.

We initialize the experiment with PSN-GRPO with **Qwen2.5-Math-7B** model. Figure 3 summarize the average performance across the evaluated datasets. We find that naive PSN-GRPO (without TIS and adaptive noise) outperforms the standard GRPO baseline when k is large (e.g., from $k = 16$ to $k = 256$). While standard RLVR improves selection efficiency among pre-existing trajectories, PSN effectively expands the reasoning search space. As shown in Figure 3, this performance boost correlates with significantly higher semantic and operation diversity compared to the baseline, confirming that PSN induces genuinely new reasoning modes rather than simply reweighting the pre-training distribution. Meanwhile, the naive PSN do hurt the pass rate when k is small. This will be mitigated through adaptive noise mechanism and answered in Question 6.

Q2: Does PSN-RLVR generalize to other models, and where Should Noise Be Injected?

A: Yes. We demonstrate that PSN is model-agnostic by training on Qwen2.5-7B and Qwen3-4B. Furthermore, both theoretical intuition and empirical results identify MLP layers as the optimal injection site for maximizing the reasoning capability boundary.

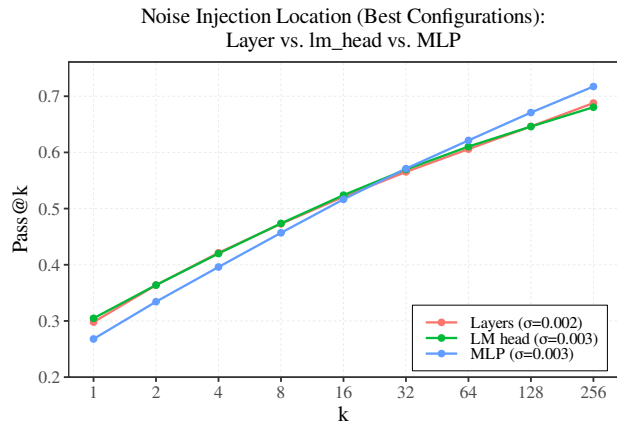


Figure 4. Noise injection location (best settings). Average pass@ k for the best noise scale at each injection place (Whole Layers, lm_head, and MLP). MLP injection attains the largest gains at high k .

Theoretical work by Plappert et al. (Plappert et al., 2018) suggests that parameter space noise yields optimal performance when using normalization between perturbed layers. In standard Transformer architectures, the MLP blocks naturally satisfy this structural criterion. To empirically validate this hypothesis and demonstrate the method’s generalization beyond specific math-tuned models, we conducted ablation studies using the general-purpose **Qwen2.5-7B** model. We compared noise injection across three distinct location: full decoding layers, the language modeling head (lm_head), and the MLP blocks. As illustrated in Figure 4, injecting noise exclusively into the MLP layers yields a superior reasoning capability boundary, demonstrating significantly higher pass@ k performance at large sampling budgets ($k \geq 128$) compared to other strategies. Comprehensive results are provided in Appendix Figure 10.

Additional evidence on Qwen3-4B-Base. We further evaluate PSN on **Qwen3-4B-Base** using our default PSN setting (MLP-only perturbation). Table 1 shows the same exploration–exploitation pattern observed in larger models: PSN slightly decreases low-budget reliability (pass@1/2) but expands the high-budget boundary (pass@256). Notably, on harder benchmarks PSN improves pass@256 on AIME24 by **+2.7pp** (62.8→65.5) and on AIME25 by **+3.7pp** (58.9→62.6), consistent with PSN unlocking additional reasoning modes under large sampling. Detailed per-benchmark results for Qwen3-4B-Base are reported in Appendix Table 7.

Q3: Is Parameter space noise more effective than action-space noise with respect to long-trajectory (CoT) reasoning in RLVR method?

Method (Qwen3-4B-Base)	Avg pass@1	Avg pass@2	Avg pass@256
Clean ($\sigma = 0$)	33.8%	41.5%	72.0%
PSN ($\sigma = 0.001$)	31.9%	40.5%	72.5%

Table 1. **Qwen3-4B-Base generalization.** Average pass@ k (%) over five math benchmarks (AIME24/25, AMC23, Minerva-Math, OlympiadBench) comparing clean decoding vs. PSN. PSN expands the high-budget reasoning boundary (avg pass@256 +0.5pp) while slightly reducing low-budget reliability, matching the exploration-exploitation trade-off.

A: Yes, parameter-space noise outperforms both **training** and **evaluation** time action-space noise by preserving long-trajectory reasoning (CoT) consistency.

We evaluate the efficacy of parameter-space exploration against action-space noise baselines. First, we compare PSN-GRPO against **training-time action-space noise**, implemented via temperature scaling ($T \in \{1.0, \dots, 1.7\}$) (Du et al., 2025). As shown in Figure 5, increasing temperature beyond 1.5 degrades performance. We attribute this failure mode to the local, unstructured nature of token-level perturbations: because action-space noise is typically uncorrelated across time steps, it accumulates into “logical drift” that disrupts the global coherence required for long-horizon Chain-of-Thought (CoT) reasoning.

In contrast, PSN perturbs the policy parameters prior to generation, inducing *trajectory-level consistency*. Consequently, PSN-GRPO demonstrates superior scaling behavior, with performance benefits becoming increasingly pronounced as the length of reasoning trajectories grow, as shown in Table 2, and detailed results are shown in Appendix Figure 7. Notably, while the performance gain over the baseline is marginal ($< 1\%$) on the shorter AMC 23 dataset (average response length is 738 tokens), the gap widens to +8.9% (pass@256) on the hard task, AIME 24 benchmark (average response length is 1,978 tokens). Furthermore, PSN-GRPO consistently exceeds the performance ceiling of **evaluation-time temperature scaling** (typically $T = 1.5$), which requires expensive tuning and lacks the coherent exploration necessary for difficult tasks as shown in Table 2, and detailed results are shown in Appendix Figure 8.

Q4: Is Truncated Importance Sampling (TIS) necessary?

A: Yes, TIS is crucial for stabilizing training by mitigating the off-policy mismatch.

Since PSN-RLVR generates rollouts using a perturbed policy π_{noisy} but updates a clean policy π_{clean} , a distribution mismatch arises. Table 3 compares standard GRPO and PSN-GRPO with and without TIS correction. We ob-

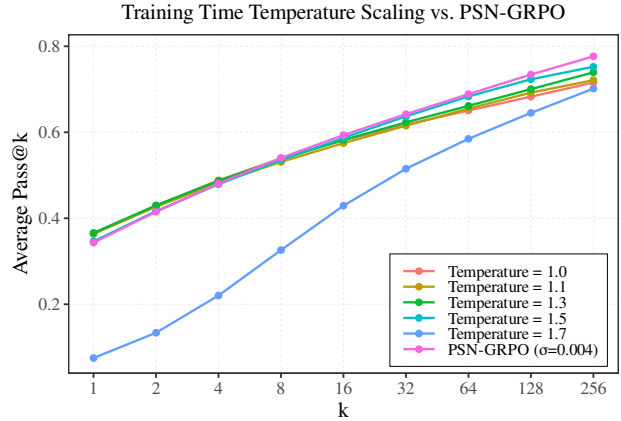


Figure 5. Average performance across benchmarks with different training time temperature. Increasing temperature beyond 1.5 degrades overall performance.

Dataset	Avg. Len (PSN)	Method	pass@64		pass@128		pass@256	
			Score	Gap	Score	Gap	Score	Gap
AMC 23	738	PSN-GRPO	96.9%	-	99.3%	-	100.0%	-
		B.Train	95.7%	+1.2%	98.5%	+0.8%	99.9%	+0.1%
		B.Eval	94.6%	+2.3%	97.0%	+2.3%	99.6%	+0.4%
Olympiad	923	PSN-GRPO	73.5%	-	77.0%	-	80.1%	-
		B.Train	72.0%	+1.5%	75.0%	+2.0%	77.9%	+2.2%
		B.Eval	72.6%	+0.9%	75.8%	+1.2%	78.7%	+1.3%
AIME 25	1030	PSN-GRPO	49.9%	-	56.1%	-	62.2%	-
		B.Train	47.3%	+2.6%	54.1%	+2.0%	61.6%	+0.6%
		B.Eval	48.6%	+1.3%	53.9%	+2.2%	61.3%	+0.9%
AIME 24	1978	PSN-GRPO	65.2%	-	73.0%	-	81.6%	-
		B.Train	64.6%	+0.6%	69.0%	+4.0%	72.7%	+8.9%
		B.Eval	58.9%	+6.3%	64.7%	+8.3%	71.7%	+9.9%

Table 2. **Performance comparison across mathematical benchmarks.** We report pass@ k scores (%) for PSN-GRPO ($\sigma = 0.004$) relative to the **best training-time** (B.Train) and **best evaluation-time** (B.Eval) temperature-scaling baselines. **Gap** denotes the absolute percentage point improvement of PSN-GRPO over the respective baseline. **Key Finding:** PSN-GRPO outperforms action-space noise by inducing *trajectory-level consistency*, effectively mitigating the logical drift observed in temperature scaling—a benefit that becomes increasingly pronounced on long-horizon tasks (e.g., AIME 24 with average response length around 2k).

serve that while TIS provides negligible benefits to standard GRPO (where the sampling and training policies are identical), it significantly boosts the performance of PSN-GRPO (e.g., increasing pass@256 from 74.33% to 76.94%). This confirms that properly handling the importance ratio clipping is essential when leveraging exploratory data from parameter-perturbed policies.

Q5: How does performance scale with noise magnitude?

A: A moderate noise level (e.g., $\sigma \in \{0.004, 0.005\}$) tends to achieve the optimal exploration-exploitation balance. While larger noise (e.g., $\sigma = 0.006$) improves pass@ k for larger k (e.g., $k = 128, 256$), it detrimentally affects performance at lower pass@ k .

Method Name	Avg of Datasets		
	pass@1	pass@128	pass@256
PSN-GRPO	36.01%	71.10%	74.33%
PSN-GRPO_with_TIS	36.15%	73.07%	76.94%

Table 3. Impact of Truncated Importance Sampling (TIS). The results show that TIS correction significantly boosts the performance of PSN-GRPO (e.g., increasing pass@256 from 74.33% to 76.94%) by effectively mitigating the off-policy mismatch between the perturbed sampling policy and the clean training policy.

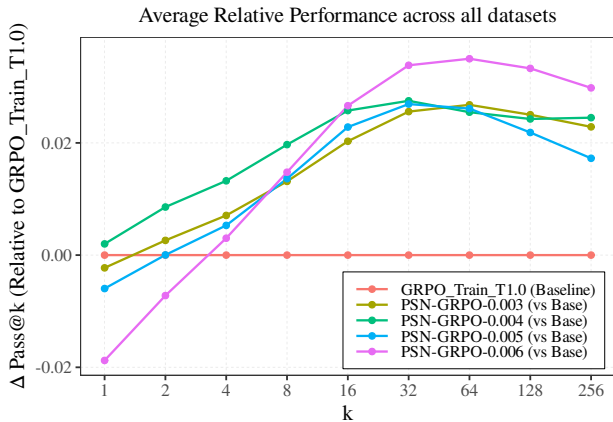


Figure 6. Impact of Noise Magnitude σ on Exploration-Exploitation. Increasing noise scale (e.g., $\sigma = 0.006$) maximizes the reasoning capability boundary at high k but degrades pass@1 performance. Moderate scales ($\sigma \in \{0.004, 0.005\}$) provide the optimal balance between exploitation reliability and exploratory diversity across benchmarks.

Figure 6 illustrates the trade-off inherent in noise magnitude selection. We find that larger noise scales (e.g., $\sigma = 0.006$) yield the highest pass@256 scores, indicating successful exploration of the outer reaches of the solution space. However, this comes at the cost of lower pass@1 performance compared to moderate noise levels (e.g., $\sigma \in \{0.004, 0.005\}$). For general applications, a moderate noise level provides the optimal balance between exploitation (reliability) and exploration (diversity).

Q6: Is adaptive noise scheduling better than fixed noise?

A: Yes, our proposed real-time certainty-aware scheduling achieves a superior exploration-stability trade-off.

We benchmark our compute-aware adaptive noise schedules (Variant I and Variant II, as detailed in Section 3.5) against fixed noise schedules and the GRPO baseline. The adaptive approach modulates σ based on semantic similarity and self-certainty signals (Equation 10). Our results highlight a critical trade-off: as shown in Table 4, and detailed result in Table 8. **Variant I** (non-real-time), despite incurring small inference overhead, suffers from feedback lag that degrades performance relative to standard GRPO. Con-

Dataset	Method	pass@2		pass@4		pass@256	
		Score	Gap	Score	Gap	Score	Gap
Average	PSN Var-II	44.1%	-	50.6%	-	79.5%	-
	GRPO Train	42.7%	+1.3%	48.7%	+1.9%	74.7%	+4.8%
	PSN Fixed	43.6%	+0.5%	50.0%	+0.6%	77.1%	+2.4%
	PSN Var-I	42.5%	+1.5%	48.7%	+1.9%	75.1%	+4.4%

Table 4. Performance comparison across mathematical benchmarks. We report pass@ k scores (%) for our adaptive variants (PSN Var-I/II) against the standard GRPO baseline and Fixed-Noise PSN ($\sigma = 0.004$). **Gap** denotes the absolute percentage point improvement of *PSN Var-II* over the compared method. Notably, the non-real-time schedule (Var-I) hurts performance due to feedback latency. In contrast, the proposed lightweight real-time schedule (Var-II) yields the best performance, improving both sample efficiency (e.g., +1.3% pass@2 vs. GRPO) and the reasoning capability boundary (e.g., +4.8% pass@256 vs. GRPO).

versely, **Variant II** (real-time), while introducing a marginal computational cost, effectively synchronizes noise scaling with the model’s current state. This results in significant gains in both sample efficiency (e.g., pass@2) and the reasoning capability boundary (e.g., pass@256), consistently outperforming both fixed-noise baselines and naive GRPO.

Q7: How does PSN-RLVR compared with other exploration methods and Is it orthogonal to these method?

A: Yes, PSN-RLVR outperforms other mainstream exploration baselines and is orthogonal to these methods, yielding additive performance gains when combined

First, we compare PSN-RLVR against two mainstreams method that increase explore capability pass@K (Chen et al., 2025) and RLVR Decomposed (Zhu et al., 2025). As illustrated in Figure 1, PSN-RLVR not only achieves a superior reasoning capability boundary (higher pass@K at large budgets) but also exhibits significantly higher semantic and operation diversity compared to the baselines. This suggests that parameter-space perturbations induce novel reasoning modes that objective or data modifications alone fail to uncover. Second, we demonstrate that PSN acts as a complementary exploration mechanism. As shown in Table 5, combining PSN with pass@K training (PSN-GRPO-pass@K) further boosts performance, improving the average pass@256 from 76.37% to 79.12% over the strong GRPO-pass@K baseline. This result confirms that PSN is orthogonal to other strategies and can be effectively composed with them to maximize exploration.

Finding: PSN-RLVR discovers qualitatively new solution strategies. To probe whether the gains in *reasoning capability boundary* reflect genuine exploration (rather than mere reweighting), we conduct an Gemini-assisted (Team,

Method Name	Avg	pass@64	pass@128	pass@256
	of Datasets			
GRPO-pass@K		69.77%	73.48%	76.37%
PSN-GRPO-pass@K		70.35%	74.82%	79.12%

Table 5. **PSN-GRPO is complementary to Pass@k training.** Combining Pass@k-based training with PSN-GRPO yields higher performance than either component alone.

2025a) qualitative analysis on AIME 2024 under our standard evaluation protocol (30 problems; $n=300$ rollouts per problem). We focus on the subset of problems where the *base/original* model fails on all 300 rollouts, yet PSN-RLVR produces at least one correct rollout. Across these cases, we find that the successful PSN-RLVR traces typically employ solution perspective that are absent from the base model’s rollout set, indicating that PSN-RLVR can access *new reasoning modes* rather than only improving selection among pre-existing trajectories. Representative examples are provided in Appendix J.

5. Limitations

PSN-RLVR is most effective for long-horizon reasoning tasks requiring global consistency. In simpler, short-sequence tasks where token-level stochasticity suffices, PSN may yield diminishing returns. This limitation is mitigated by our real-time adaptive scheduler (Table 8), though further investigation is warranted.

6. Conclusion

We introduced PSN-RLVR, the first systematic study of parameter-space noise for RLVR-trained language models, motivated by the observation that standard RLVR can saturate, primarily by improving selection among already-likely trajectories. By perturbing parameters (rather than tokens) to produce rollout-consistent exploration, PSN-RLVR improves long-horizon reasoning and yields larger gains under high sampling budgets. We showed that injecting noise into Transformer MLP/FFN blocks offers a favorable stability–exploration trade-off, and that truncated importance sampling is essential to reliably exploit exploratory data from perturbed policies. Finally, our lightweight certainty- and semantics-aware scheduling achieves robust performance without additional rollout overhead, and PSN composes with existing RLVR exploration strategies to further extend the achievable pass@k frontier.

Impact Statement

This work advances RLVR for reasoning by introducing a practical exploration mechanism—parameter-space noise with stable off-policy correction and compute-aware scheduling—that improves high-budget sampling perfor-

mance and diversity on verifiable math benchmarks. The primary positive impact is enabling more reliable and efficient discovery of correct solution strategies in domains with automated checkers (e.g., education and software tooling). As with other stronger reasoning models, misuse risks include facilitating automated generation of deceptive content or enabling harmful applications; our method does not inherently mitigate these risks. We recommend standard safeguards for model deployment, including controlled access, monitoring, and domain-specific evaluation beyond verifiable tasks.

References

- Aime. aime problems and solutions,, 2025. URL https://artofproblemsolving.com/wiki/index.php/AIME_Problems_and_Solutions.
- Amini, A., Vieira, T., and Cotterell, R. Better estimation of the kullback–leibler divergence between language models, 2025. URL <https://arxiv.org/abs/2504.10637>.
- Aravindan, S. and Lee, W. S. State-aware variational thompson sampling for deep q-networks. In *AAMAS ’21: 20th International Conference on Autonomous Agents and Multiagent Systems*, pp. 124–132. ACM, 2021. doi: 10.5555/3463952.3463973.
- Chen, A., Phang, J., Parrish, A., Padmakumar, V., Zhao, C., Bowman, S. R., and Cho, K. Two failures of self-consistency in the multi-step reasoning of llms, 2024. URL <https://arxiv.org/abs/2305.14279>.
- Chen, Z., Qin, X., Wu, Y., Ling, Y., Ye, Q., Zhao, W. X., and Shi, G. Pass@k training for adaptively balancing exploration and exploitation of large reasoning models. *ArXiv*, abs/2508.10751, 2025. URL <https://api.semanticscholar.org/CorpusID:280649795>.
- Cheng, D., Huang, S., Zhu, X., Dai, B., Zhao, W. X., Zhang, Z., and Wei, F. Reasoning with exploration: An entropy perspective, 2025a. URL <https://arxiv.org/abs/2506.14758>.
- Cheng, R., Zhou, K., Wei, X., Liu, S., Han, M., Ai, M., Zhou, Y., Zhong, B., Xiao, W., Chen, R., and Chen, H. Fast llm post-training via decoupled and fastest-of-n speculation, 2025b. URL <https://arxiv.org/abs/2511.16193>.
- Cobbe, K., Kosaraju, V., Bavarian, M., Chen, M., Jun, H., Kaiser, L., Plappert, M., Tworek, J., Hilton, J., Nakano, R., Hesse, C., and Schulman, J. Training verifiers to solve math word problems, 2021. URL <https://arxiv.org/abs/2110.14168>.

- Cui, G., Zhang, Y., Chen, J., Yuan, L., Wang, Z., Zuo, Y., Li, H., Fan, Y., Chen, H., Chen, W., Liu, Z., Peng, H., Bai, L., Ouyang, W., Cheng, Y., Zhou, B., and Ding, N. The entropy mechanism of reinforcement learning for reasoning language models, 2025. URL <https://arxiv.org/abs/2505.22617>.
- Dang, X., Baek, C., Kolter, J. Z., and Raghunathan, A. Assessing diversity collapse in reasoning. In *ICLR 2025 Workshop on Scaling Self-Improving Foundation Models without Human Supervision (SSI-FM)*, 2025. URL <https://openreview.net/forum?id=AMiKsHLjQh>.
- Dong, Y., Jiang, X., Tao, Y., Liu, H., Zhang, K., Mou, L., Cao, R., Ma, Y., Chen, J., Li, B., Jin, Z., Huang, F., Li, Y., and Li, G. RI-plus: Countering capability boundary collapse of llms in reinforcement learning with hybrid-policy optimization, 2025. URL <https://arxiv.org/abs/2508.00222>.
- Du, W., Yang, Y., and Welleck, S. Optimizing temperature for language models with multi-sample inference, 2025. URL <https://arxiv.org/abs/2502.05234>.
- Fang, L., Wang, Y., Liu, Z., Zhang, C., Jegelka, S., Gao, J., Ding, B., and Wang, Y. What is wrong with perplexity for long-context language modeling?, 2025. URL <https://arxiv.org/abs/2410.23771>.
- Fortunato, M., Azar, M. G., Piot, B., Menick, J., Osband, I., Graves, A., Mnih, V., Munos, R., Hassabis, D., Legg, S., et al. Noisy networks for exploration. In *International Conference on Learning Representations (ICLR)*, 2018. arXiv:1706.10295.
- Gravell, B. and Summers, T. Robust learning-based control via bootstrapped multiplicative noise, 2021. URL <https://arxiv.org/abs/2002.10069>.
- Guo, D., Yang, D., Zhang, H., Song, J., Wang, P., Zhu, Q., Xu, R., Zhang, R., Ma, S., Bi, X., Zhang, X., Yu, X., Wu, Y., Wu, Z. F., Gou, Z., Shao, Z., Li, Z., Gao, Z., Liu, A., Xue, B., Wang, B., Wu, B., Feng, B., Lu, C., Zhao, C., Deng, C., Ruan, C., Dai, D., Chen, D., Ji, D., Li, E., Lin, F., Dai, F., Luo, F., Hao, G., Chen, G., Li, G., Zhang, H., Xu, H., Ding, H., Gao, H., Qu, H., Li, H., Guo, J., Li, J., Chen, J., Yuan, J., Tu, J., Qiu, J., Li, J., Cai, J. L., Ni, J., Liang, J., Chen, J., Dong, K., Hu, K., You, K., Gao, K., Guan, K., Huang, K., Yu, K., Wang, L., Zhang, L., Zhao, L., Wang, L., Zhang, L., Xu, L., Xia, L., Zhang, M., Zhang, M., Tang, M., Zhou, M., Li, M., Wang, M., Li, M., Tian, N., Huang, P., Zhang, P., Wang, Q., Chen, Q., Du, Q., Ge, R., Zhang, R., Pan, R., Wang, R., Chen, R. J., Jin, R. L., Chen, R., Lu, S., Zhou, S., Chen, S., Ye, S., Wang, S., Yu, S., Zhou, S., Pan, S., Li, S. S., Zhou, S., Wu, S., Yun, T., Pei, T., Sun, T., Wang, T., Zeng, W., Liu, W., Liang, W., Gao, W., Yu, W., Zhang, W., Xiao, W. L., An, W., Liu, X., Wang, X., Chen, X., Nie, X., Cheng, X., Liu, X., Xie, X., Liu, X., Yang, X., Li, X., Su, X., Lin, X., Li, X. Q., Jin, X., Shen, X., Chen, X., Sun, X., Wang, X., Song, X., Zhou, X., Wang, X., Shan, X., Li, Y. K., Wang, Y. Q., Wei, Y. X., Zhang, Y., Xu, Y., Li, Y., Zhao, Y., Sun, Y., Wang, Y., Yu, Y., Zhang, Y., Shi, Y., Xiong, Y., He, Y., Piao, Y., Wang, Y., Tan, Y., Ma, Y., Liu, Y., Guo, Y., Ou, Y., Wang, Y., Gong, Y., Zou, Y., He, Y., Xiong, Y., Luo, Y., You, Y., Liu, Y., Zhou, Y., Zhu, Y. X., Huang, Y., Li, Y., Zheng, Y., Zhu, Y., Ma, Y., Tang, Y., Zha, Y., Yan, Y., Ren, Z. Z., Ren, Z., Sha, Z., Fu, Z., Xu, Z., Xie, Z., Zhang, Z., Hao, Z., Ma, Z., Yan, Z., Wu, Z., Gu, Z., Zhu, Z., Liu, Z., Li, Z., Xie, Z., Song, Z., Pan, Z., Huang, Z., Xu, Z., Zhang, Z., and Zhang, Z. Deepseek-r1 incentivizes reasoning in llms through reinforcement learning. *Nature*, 645(8081):633–638, September 2025. ISSN 1476-4687. doi: 10.1038/s41586-025-09422-z. URL <http://dx.doi.org/10.1038/s41586-025-09422-z>.
- Gupta, A., Mendonca, R., Liu, Y., Abbeel, P., and Levine, S. Meta-reinforcement learning of structured exploration strategies. In *Neural Information Processing Systems*, 2018. URL <https://api.semanticscholar.org/CorpusID:3418899>.
- He, C., Luo, R., Bai, Y., Hu, S., Thai, Z., Shen, J., Hu, J., Han, X., Huang, Y., Zhang, Y., et al. Olympiadbench: A challenging benchmark for promoting agi with olympiad-level bilingual multimodal scientific problems. In *Proceedings of the 62nd Annual Meeting of the Association for Computational Linguistics (Volume 1: Long Papers)*, pp. 3828–3850, 2024.
- He, J., Li, T., Feng, E., Du, D., Liu, Q., Liu, T., Xia, Y., and Chen, H. History rhymes: Accelerating llm reinforcement learning with rhymerl, 2025. URL <https://arxiv.org/abs/2508.18588>.
- Hendrycks, D., Burns, C., Kadavath, S., Arora, A., Basart, S., Tang, E., Song, D., and Steinhardt, J. Measuring mathematical problem solving with the math dataset. *arXiv preprint arXiv:2103.03874*, 2021.
- Hollenstein, J. J., Auddy, S., Saveriano, M., Renaudo, E., and Piater, J. H. Action noise in off-policy deep reinforcement learning: Impact on exploration and performance. *ArXiv*, abs/2206.03787, 2022. URL <https://api.semanticscholar.org/CorpusID:249461896>.
- Holtzman, A., Buys, J., Du, L., Forbes, M., and Choi, Y. The curious case of neural text degeneration. *ArXiv*, abs/1904.09751, 2019. URL <https://api.semanticscholar.org/CorpusID:127986954>.

- Huang, W., Ge, Y., Yang, S., Xiao, Y., Mao, H., Lin, Y., Ye, H., Liu, S., Cheung, K. C., Yin, H., Lu, Y., Qi, X., Han, S., and Chen, Y. Qerl: Beyond efficiency – quantization-enhanced reinforcement learning for llms, 2025. URL <https://arxiv.org/abs/2510.11696>.
- Ionides, E. L. Truncated importance sampling. *Journal of Computational and Graphical Statistics*, 17(2):295–311, 2008. doi: 10.1198/106186008X320456.
- Jiang, Z., Han, J., Li, T., Wang, X., Jiang, S., Liang, J., Dai, Z., Ma, S., Yu, F., and Xiao, Y. Selective expert guidance for effective and diverse exploration in reinforcement learning of llms, 2025. URL <https://arxiv.org/abs/2510.04140>.
- Kang, Z., Zhao, X., and Song, D. Scalable best-of-n selection for large language models via self-certainty, 2025. URL <https://arxiv.org/abs/2502.18581>.
- Lambert, N., Morrison, J., Pyatkin, V., Huang, S., Ivison, H., Brahman, F., Miranda, L. J. V., Liu, A., Dziri, N., Lyu, S., Gu, Y., Malik, S., Graf, V., Hwang, J. D., Yang, J., Bras, R. L., Tafford, O., Wilhelm, C., Soldaini, L., Smith, N. A., Wang, Y., Dasigi, P., and Hajishirzi, H. Tulu 3: Pushing frontiers in open language model post-training, 2025. URL <https://arxiv.org/abs/2411.15124>.
- Langley, P. Crafting papers on machine learning. In Langley, P. (ed.), *Proceedings of the 17th International Conference on Machine Learning (ICML 2000)*, pp. 1207–1216, Stanford, CA, 2000. Morgan Kaufmann.
- Lewkowycz, A., Andreassen, A., Dohan, D., Dyer, E., Michalewski, H., Ramasesh, V., Slone, A., Anil, C., Schlag, I., Gutman-Solo, T., et al. Solving quantitative reasoning problems with language models. *Advances in neural information processing systems*, 35:3843–3857, 2022.
- LI, J., Beeching, E., Tunstall, L., Lipkin, B., Solteskyi, R., Huang, S. C., Rasul, K., Yu, L., Jiang, A., Shen, Z., Qin, Z., Dong, B., Zhou, L., Fleureau, Y., Lample, G., and Polu, S. Numina-math. [<https://huggingface.co/AI-MO/NuminaMath-CoT>] (https://github.com/project-numina/aimo-progress-prize/blob/main/report/numina_dataset.pdf), 2024.
- Li, J., Lin, H., Lu, H., Wen, K., Yang, Z., Gao, J., Wu, Y., and Zhang, J. Questa: Expanding reasoning capacity in llms via question augmentation, 2025. URL <https://arxiv.org/abs/2507.13266>.
- Liang, X., Li, Z., Gong, Y., Shen, Y., Wu, Y. N., Guo, Z., and Chen, W. Beyond pass@1: Self-play with variational problem synthesis sustains rlvr, 2025. URL <https://arxiv.org/abs/2508.14029>.
- Lu, P., Bansal, H., Xia, T., Liu, J., Li, C., Hajishirzi, H., Cheng, H., Chang, K.-W., Galley, M., and Gao, J. Mathvista: Evaluating mathematical reasoning of foundation models in visual contexts, 2024. URL <https://arxiv.org/abs/2310.02255>.
- Osband, I., Van Roy, B., Russo, D. J., and Wen, Z. Deep exploration via randomized value functions. *Journal of Machine Learning Research*, 20(124):1–62, 2019.
- Ouyang, L. et al. Training language models to follow instructions with human feedback. *Advances in Neural Information Processing Systems*, 35:27730–27744, 2022.
- Peng, R., Ren, Y., Yu, Z., Liu, W., and Wen, Y. Simko: Simple pass@k policy optimization, 2025. URL <https://arxiv.org/abs/2510.14807>.
- Plappert, M., Houthoofd, R., Dhariwal, P., Sidor, S., Chen, R. Y., Chen, X., Asfour, T., Abbeel, P., and Andrychowicz, M. Parameter space noise for exploration. In *International Conference on Learning Representations*, 2018.
- Qiang, Y., Nandi, S., Mehrabi, N., Steeg, G. V., Kumar, A., Rumshisky, A., and Galstyan, A. Prompt perturbation consistency learning for robust language models, 2024. URL <https://arxiv.org/abs/2402.15833>.
- Renze, M. and Guven, E. The effect of sampling temperature on problem solving in large language models. *ArXiv*, abs/2402.05201, 2024. URL <https://api.semanticscholar.org/CorpusID:267547769>.
- Russo, D. Worst-case regret bounds for exploration via randomized value functions. In *Advances in Neural Information Processing Systems (NeurIPS)*, volume 32, pp. 14410–14420, 2019.
- Schulman, J., Wolski, F., Dhariwal, P., Radford, A., and Klimov, O. Proximal policy optimization algorithms, 2017. URL <https://arxiv.org/abs/1707.06347>.
- Sheng, G., Zhang, C., Ye, Z., Wu, X., Zhang, W., Zhang, R., Peng, Y., Lin, H., and Wu, C. Hybridflow: A flexible and efficient rlhf framework. *arXiv preprint arXiv:2409.19256*, 2024.
- Shi, C., Yang, H., Cai, D., Zhang, Z., Wang, Y., Yang, Y., and Lam, W. A thorough examination of decoding methods in the era of llms. In *Conference on Empirical Methods in Natural Language Processing*, 2024. URL <https://api.semanticscholar.org/CorpusID:267627384>.

- Shur-Ofry, M., Horowitz-Amsalem, B., Rahamim, A., and Belinkov, Y. Growing a tail: Increasing output diversity in large language models. *ArXiv*, abs/2411.02989, 2024. URL <https://api.semanticscholar.org/CorpusID:273821765>.
- Steinfeldt, C. and Mihaljevic, H. Bert-MLM_arXiv-MP-class_zbMath: A sentence-transformers model for similarity of short mathematical texts. https://huggingface.co/math-similarity/Bert-MLM_arXiv-MP-class_zbMath, 2024. Hugging Face model card. Accessed: 2026-01-25.
- Sutton, R. S. and Barto, A. G. Reinforcement learning: An introduction. *IEEE Trans. Neural Networks*, 9:1054–1054, 1998. URL <https://api.semanticscholar.org/CorpusID:60035920>.
- Team, G. Gemini 2.5: Pushing the frontier with advanced reasoning, multimodality, long context, and next generation agentic capabilities. *ArXiv*, abs/2507.06261, 2025a. URL <https://api.semanticscholar.org/CorpusID:280151524>.
- Team, Q. Qwen2.5 technical report, 2025b. URL <https://arxiv.org/abs/2412.15115>.
- Wu, F., Xuan, W., Lu, X., Liu, M., Dong, Y., Harchaoui, Z., and Choi, Y. The invisible leash: Why rlvr may or may not escape its origin, 2026. URL <https://arxiv.org/abs/2507.14843>.
- Yang, A., Zhang, B., Hui, B., Gao, B., Yu, B., Li, C., Liu, D., Tu, J., Zhou, J., Lin, J., Lu, K., Xue, M., Lin, R., Liu, T., Ren, X., and Zhang, Z. Qwen2.5-math technical report: Toward mathematical expert model via self-improvement, 2024. URL <https://arxiv.org/abs/2409.12122>.
- Yue, Y., Chen, Z., Lu, R., Zhao, A., Wang, Z., Yue, Y., Song, S., and Huang, G. Does reinforcement learning really incentivize reasoning capacity in llms beyond the base model?, 2025. URL <https://arxiv.org/abs/2504.13837>.
- Zeng, W., Huang, Y., Liu, Q., Liu, W., He, K., Ma, Z., and He, J. Simplerl-zoo: Investigating and taming zero reinforcement learning for open base models in the wild, 2025. URL <https://arxiv.org/abs/2503.18892>.
- Zhan, G., Wang, L., Wang, P., Zhang, F., Duan, J., Tomizuka, M., and Li, S. E. Mind your entropy: From maximum entropy to trajectory entropy-constrained rl. *ArXiv*, abs/2511.11592, 2025. URL <https://api.semanticscholar.org/CorpusID:283071650>.
- Zhu, X., Xia, M., Wei, Z., Chen, W.-L., Chen, D., and Meng, Y. The surprising effectiveness of negative reinforcement in llm reasoning, 2025. URL <https://arxiv.org/abs/2506.01347>.

A. Related works for Reinforcement Learning for Reasoning with Verifiable Rewards

The integration of Reinforcement Learning (RL) into the post-training pipeline of Large Language Models (LLMs) has become a standard paradigm for enhancing performance in domains with objective ground-truth, such as mathematics and coding (Ouyang et al., 2022; Lu et al., 2024). Early approaches primarily utilized Proximal Policy Optimization (PPO) (?) to align models with reward signals derived from unit tests or symbolic solvers. More recently, Group Relative Policy Optimization (GRPO) (Guo et al., 2025) has gained prominence by eliminating the need for a separate value network, instead normalizing advantages within a group of sampled outputs. This efficiency has enabled massive-scale RL training, exemplified by models like DeepSeek-R1, which demonstrate emergent reasoning capabilities solely through reinforcement signals. However, emerging evidence suggests that current RLVR pipelines may face an *exploration ceiling*. Recent analyses (Yue et al., 2025; Wu et al., 2026) show that RLVR predominantly improves *selection efficiency* among pre-existing trajectories, with limited ability to generate genuinely new reasoning modes, leaving the learned policy largely constrained by the base model’s pretraining distribution and exposing a critical exploration bottleneck.

B. Training experiment setting

Table 6. Hyperparameters used for SimpleRL-Zoo models.

Settings	SimpleRL-Zoo
Framework	verl (Sheng et al., 2024)
Prompt Batch Size	512
Mini-batch Size	256
# Policy Rollout G	8
Max Rollout Length	8,192
Max Generation Length (Eval)	16,384
Clip Ratio	0.2
KL Loss Coefficient	1×10^{-4}
Training Temperature	1.0
Evaluation Temperature	0.9
Adaptive Noise Update Step β	1.01
Adaptive Noise Scale Range	$[0.8\sigma_{\text{init}}, 1.2\sigma_{\text{init}}]$
Target Divergence δ	0.03
C in TIS Equation 4	10

C. Compute overhead.

Variant II uses two probe generations per query under π_θ to estimate semantic similarity and self-certainty before sampling the G training rollouts under $\pi_{\hat{\theta}}$. With $G = 8$, a naive upper-bound estimate suggests $2/8 = 0.25$ additional generations time; if on-policy rollout generation occupies at least 70% of wall-clock training time, this would imply an expected slowdown of roughly $0.25 \times 0.70 \approx 0.17$ (i.e., $\approx 17\%$). Empirically, however, we observe a smaller end-to-end throughput reduction of per-iteration $\approx 8\%$ relative to fixed- σ PSN under identical hardware, batch size, and maximum generation length. We attribute the gap to *generation-time imbalance* (He et al., 2025): in batched/parallel decoding, shorter sequences finish earlier and GPUs can become partially idle while waiting for the longest sequences (stragglers) to complete. Adding a small number of short probe generations reduces the variance in per-step generation workload and mitigates tail-latency effects, leading to a wall-clock overhead that is lower than the token-count-based estimate.

D. Result of Qwen3-4B-Base

Benchmark	Clean ($\sigma = 0$)			PSN ($\sigma = 0.001$)			Gap (PSN–Clean)		
	pass@1	pass@2	pass@256	pass@1	pass@2	pass@256	pass@1	pass@2	pass@256
AIME 24	19.4%	25.7%	62.8%	17.4%	23.6%	65.5%	-2.0	-2.1	+2.7
AIME 25	15.5%	20.6%	58.9%	14.7%	20.0%	62.6%	-0.8	-0.6	+3.7
Minerva-Math	32.2%	39.3%	63.6%	32.0%	40.7%	64.8%	-0.2	+1.4	+1.2
OlympiadBench	44.4%	52.9%	77.1%	40.6%	50.8%	77.4%	-3.8	-2.1	+0.3

Table 7. **Qwen3-4B-Base detailed results (clean vs. PSN)**. Per-benchmark pass@ k (%) for Qwen3-4B-Base comparing clean decoding ($\sigma = 0$) and PSN ($\sigma = 0.001$; MLP-only perturbation). PSN exhibits the typical exploration–exploitation trade-off: slightly lower low-budget reliability (pass@1/2) but an expanded high-budget capability boundary (pass@256), especially on harder AIME benchmarks.

E. Detailed performance of training time temperature scaling

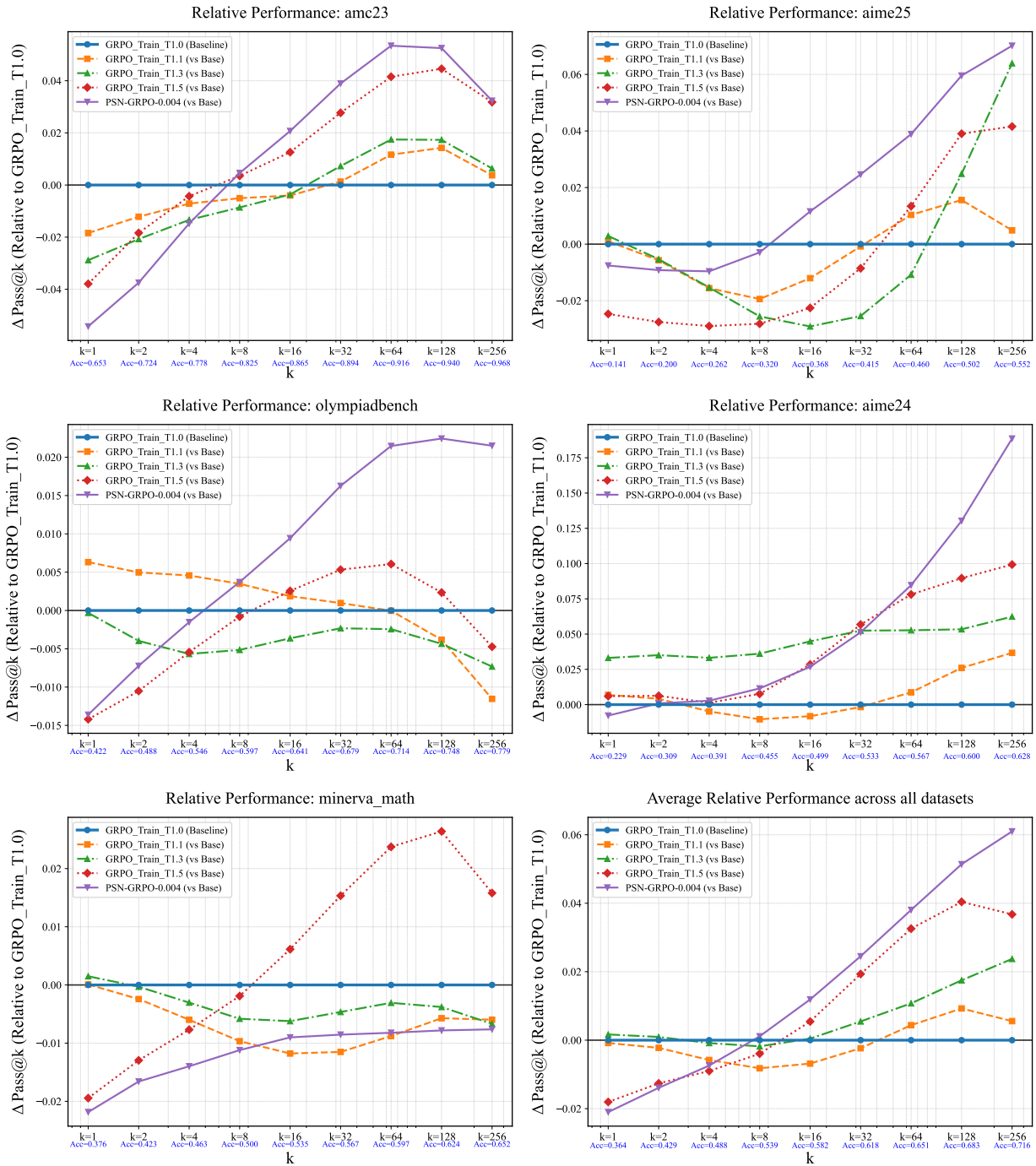


Figure 7. Performance across benchmarks. We do not plot $T=1.7$ in these plots since its overall performance collapsed as shown in Figure 5.

F. More experiment result of evaluation temperature scaling

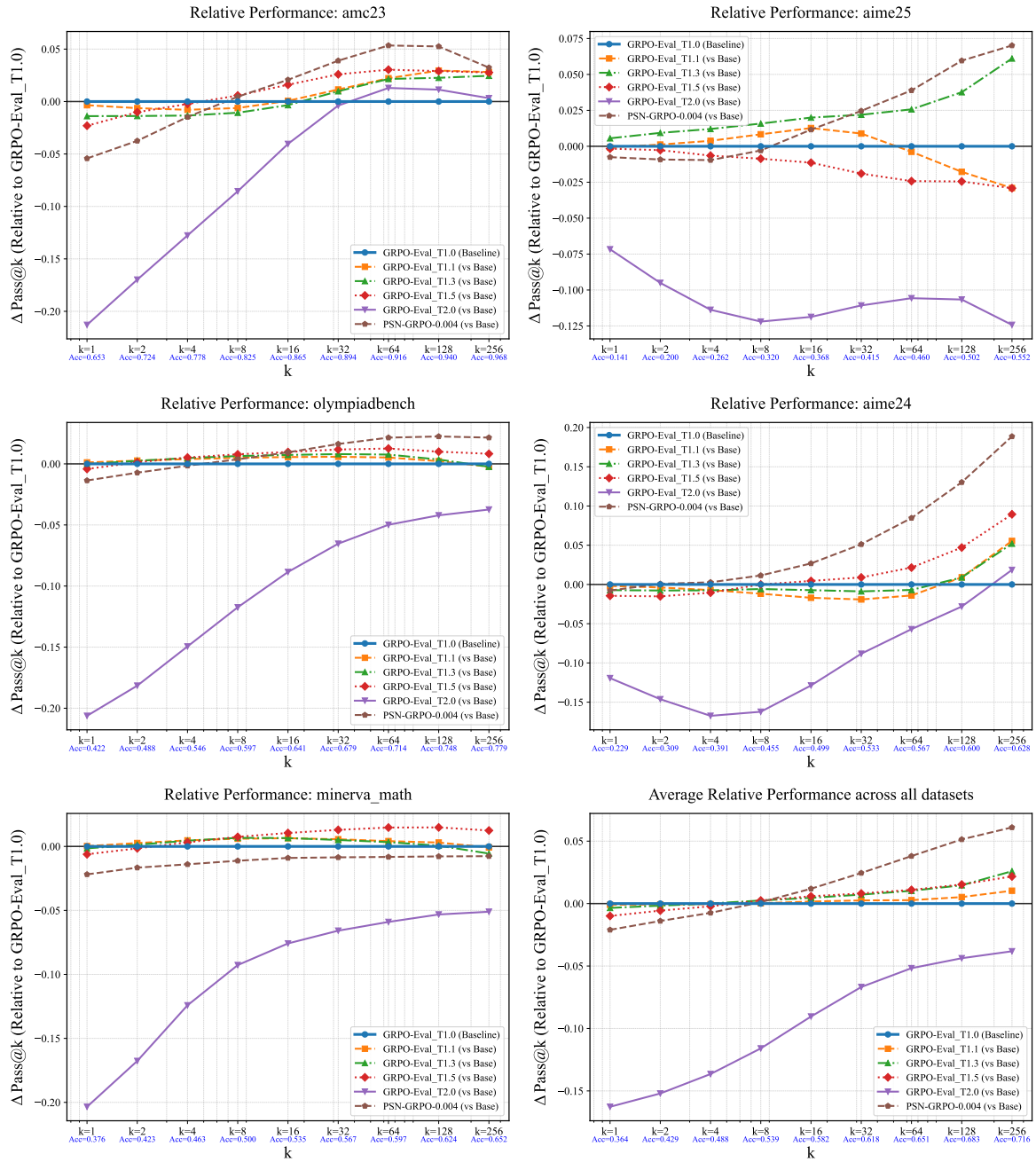


Figure 8. Detailed performance analysis across five datasets.

G. More detailed experiment result of evaluation temperature scaling

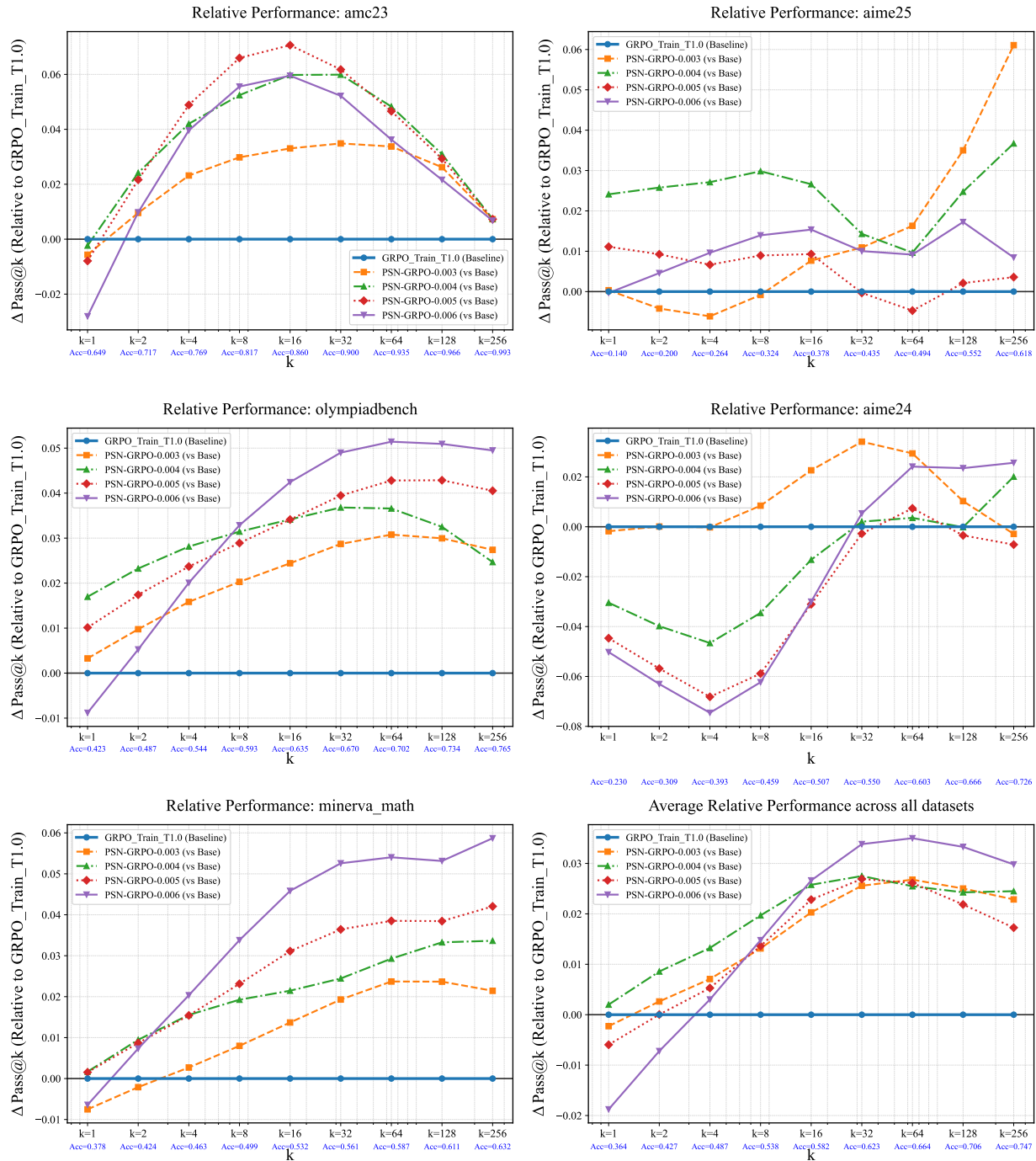


Figure 9. Detailed performance analysis across five datasets. In general, a larger noise scale σ tends to yield higher pass@ k for large k . Specifically, on datasets of moderate difficulty (e.g., OlympiadBench and Minerva Math), increased σ improves reasoning capability boundary, yield higher pass@ k for large k . Conversely, on more challenging benchmarks such as AIME24 and AIME25, a larger noise scale tends to degrade overall performance.

H. Detailed performance of where to inject noise

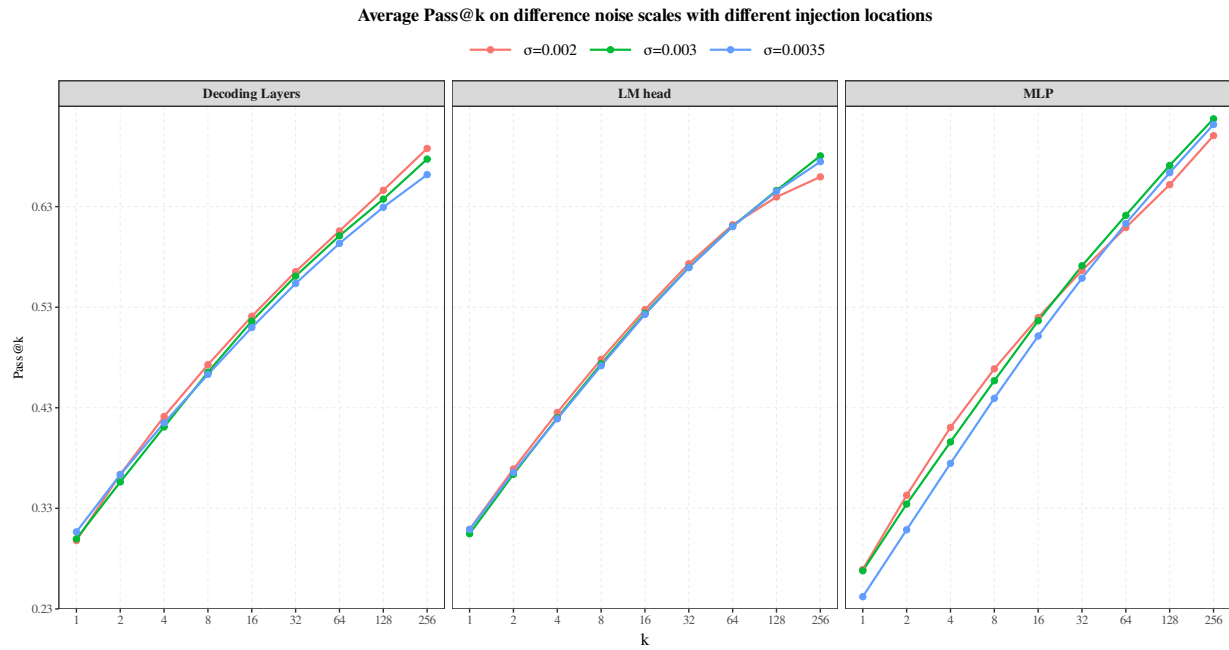


Figure 10. Average Pass@k under parameter-space noise injected whole transformer layers, the `lm_head`, or all MLP sublayers, sweeping noise scale σ . MLP injection yields the strongest and most consistent improvements, especially at large k .

I. Detailed performance of adaptive noise

Dataset	Method	Pass@2		Pass@4		Pass@256	
		Score	Gap	Score	Gap	Score	Gap
AMC 23	PSN Var-II	74.3%	-	81.8%	-	99.6%	-
	GRPO Train	71.7%	+2.6%	76.9%	+4.8%	99.3%	+0.4%
	PSN Fixed	74.1%	+0.2%	81.1%	+0.6%	100.0%	-0.4%
	PSN Var-I	72.6%	+1.7%	79.2%	+2.6%	100.0%	-0.4%
Olympiad	PSN Var-II	51.3%	-	57.7%	-	81.1%	-
	GRPO Train	48.7%	+2.6%	54.4%	+3.3%	76.5%	+4.7%
	PSN Fixed	51.1%	+0.3%	57.2%	+0.5%	78.9%	+2.2%
	PSN Var-I	50.3%	+1.0%	56.4%	+1.3%	78.6%	+2.6%
AIME 25	PSN Var-II	22.9%	-	29.2%	-	65.8%	-
	GRPO Train	20.0%	+2.9%	26.4%	+2.8%	61.8%	+4.0%
	PSN Fixed	22.6%	+0.3%	29.1%	+0.1%	65.4%	+0.3%
	PSN Var-I	20.7%	+2.2%	26.9%	+2.3%	55.1%	+10.7%
AIME 24	PSN Var-II	28.1%	-	37.1%	-	81.7%	-
	GRPO Train	30.9%	-2.8%	39.3%	-2.2%	72.6%	+9.1%
	PSN Fixed	27.0%	+1.1%	34.6%	+2.4%	74.6%	+7.1%
	PSN Var-I	25.5%	+2.6%	32.9%	+4.2%	75.0%	+6.7%
Minerva	PSN Var-II	43.7%	-	47.4%	-	69.1%	-
	GRPO Train	42.4%	+1.4%	46.3%	+1.0%	63.2%	+5.9%
	PSN Fixed	43.3%	+0.4%	47.9%	-0.5%	66.6%	+2.5%
	PSN Var-I	43.5%	+0.3%	48.0%	-0.7%	66.7%	+2.4%
Average	PSN Var-II	44.1%	-	50.6%	-	79.5%	-
	GRPO Train	42.7%	+1.3%	48.7%	+1.9%	74.7%	+4.8%
	PSN Fixed	43.6%	+0.5%	50.0%	+0.6%	77.1%	+2.4%
	PSN Var-I	42.5%	+1.5%	48.7%	+1.9%	75.1%	+4.4%

Table 8. **Performance comparison across mathematical benchmarks.** We report Pass@ k scores (%) for our adaptive variants (PSN Var-I/II) against the standard GRPO baseline and Fixed-Noise PSN ($\sigma = 0.004$). **Gap** denotes the absolute percentage point improvement of *PSN Var-II* over the compared method. Notably, the non-real-time schedule (Var-I) hurts performance due to feedback latency.

J. Detailed example of PSN-GRPO discovers qualitatively new solution strategies

Question (AIME I 2024, Problem 6)

Each vertex of a regular octagon is independently colored either red or blue with equal probability. The probability that the octagon can then be rotated so that all of the blue vertices end up at positions where there were originally red vertices is $\frac{m}{n}$, where m and n are relatively prime positive integers. What is $m + n$?

✗ Baseline Error Logic 1: Invariance Trap

The model incorrectly simplifies the problem by assuming the coloring must be invariant under a non-trivial rotation.

- It identifies $k \in \{0, 4, 8\}$ as the only counts allowing rotation.
- For $k = 4$, it only counts 2 symmetric patterns (alternating positions $\{1, 3, 5, 7\}$ and $\{2, 4, 6, 8\}$).

Total colorings = $1(k = 0) + 2(k = 4) + 1(k = 8) = 4$.

Diversity Collapse: The policy has collapsed to a small subset of globally symmetric solutions. It fails to recognize that “rotatable to red” simply requires the set of blue vertices B to satisfy $B \cap R_\theta(B) = \emptyset$ for at least one θ .

✗ Baseline Error Logic 2: Local Symmetry Constraint

For $k = 2$, the model argues that if vertices are at positions $\{1, 3\}$, they cannot be rotated because “the 90° separation does not align with the octagon’s fundamental 45° or 180° symmetry axis.” It erroneously prunes all non-opposite pairs.

Exploration Ceiling: This demonstrates a failure to simulate even a single-step 45° rotation ($1 \rightarrow 2, 3 \rightarrow 4$). The model incorrectly filters out valid configurations that do not satisfy its rigid internal symmetry priors, leading to a massive undercount.

✗ Baseline Error Logic 3: Counting Pruning Error

For $k = 3$ and $k = 4$, the model bypasses enumeration entirely. It claims that since $k \geq 3$ creates “too many constraints on adjacent slots,” it is statistically impossible for a rotation to map all blue vertices to red positions unless the distribution is perfectly uniform (i.e., the $k = 4$ case in Error 1).

Reasoning Failure: The model uses pigeonhole-style heuristics incorrectly. It fails to explore asymmetric but valid sparse placements (e.g., $k = 3$ with no two adjacent). PSN-GRPO finds 40 and 46 cases for $k = 3, 4$, which the baseline misses due to premature search pruning.

✓ PSN-GRPO Answer (Ours)

PSN-GRPO identifies the problem’s core requirement: finding all $B \subseteq V$ such that $\exists \theta \in \{45^\circ, \dots, 315^\circ\}, R_\theta(B) \cap B = \emptyset$.

Comprehensive Strategy Discovery:

- $k = 0, 1$: All $\binom{8}{0} + \binom{8}{1} = 9$ colorings work.
- $k = 2$: Valid if not adjacent ($B = \{1, 2\}$ fails for all θ). Valid = $\binom{8}{2} - 8 = 20$.
- $k = 3$: PSN explores non-symmetric triplets. It correctly excludes triplets like $\{1, 2, 3\}$ and $\{1, 2, x\}$ where all rotations are blocked. Valid = $\binom{8}{3} - 16 = 40$.
- $k = 4$: Discovers 46 valid cases by maintaining diverse reasoning paths that avoid the “greedy trap” of symmetry.

Strategic Discovery: PSN-GRPO’s parameter-space perturbation allows it to sustain multiple valid reasoning trajectories for complex counts ($k = 3, 4$), eventually summing to 115 favorable colorings.

Total Probability = $115/256$. Result: $m + n = 115 + 256 = \mathbf{371}$.